Slice-Less Optical Arbitrary Waveform Measurement (OAWM) in a Bandwidth of More Than 600 GHz

Daniel Drayss[1,2], Dengyang Fang[2], Christoph Füllner[2], Grigorii Likhachev[3], Thomas Henauer[4], Yung Chen[2], Huanfa Peng[2], Pablo Marin-Palomo[2], Thomas Zwick[4], Wolfgang Freude[2], Tobias J. Kippenberg[3], Sebastian Randel[2], and Christian Koos[1,2]

(1) Institute of Microstructure Technology (IMT), Karlsruhe Institute of Technology, 76344 Eggenstein-Leopoldshafen, Germany
(2) Institute of Photonics and Quantum Electronics (IPQ), Karlsruhe Institute of Technology, 76131 Karlsruhe, Germany
(3) Institute of Physics, Swiss Federal Institute of Technology Lausanne (EPFL), CH-1015 Lausanne, Switzerland
(4) Institute of Radio Frequency Engineering and Electronics (IHE), Karlsruhe Institute of Technology, 76131 Karlsruhe, Germany
daniel.drayss@kit.edu, christain.koos@kit.edu

Abstract: We demonstrate an optical arbitrary waveform measurement (OAWM) technique that exploits optical frequency combs as multi-wavelength local oscillators (LO) and that does not require any optical slicing filters. In a proof-of-concept experiment, we achieve record-high bandwidths exceeding 600 GHz. © 2022 The Author(s)

1. Introduction

Optical arbitrary waveform measurement (OAWM) based on frequency combs [1-3] has the potential to unlock a wide variety of applications, ranging from reception of high-speed data signals [2-5] and elastic optical networking [6] to investigation of ultra-short events and photonic-electronic analog-to-digital conversion (ADC) [7-8]. Previous demonstrations of OAWM relied on spectrally sliced coherent detection [1-3], where optical filters are used to decompose a broadband signal into several spectral slices, that are individually detected by an array of in-phase/quadrature receivers (IQR) using a frequency comb as multi-wavelength local oscillator (LO). The reconstruction of the optical waveform then relies on precise stitching of the spectral slices through digital signal processing (DSP). Based on this concept, OAWM of a 228 GHz-wide signal was demonstrated using discrete components [2], and further work demonstrated a 320 GHz photonic-electronic ADC that combines spectrally sliced OAWM with high-speed electro-optic modulators [7]. However, all these schemes crucially rely on high-quality optical filters for spectral slicing of the optical signal and for separating the comb tones. These filters lead to additional insertion loss and render the overall schemes difficult to miniaturize, in particular when relying on high index-contrast integration platforms such as indium phosphide (InP) or silicon photonics. Therefore, integrated OAWM systems had to either rely on phase-error-correction of the underlying arrayed waveguide gratings (AWG) [9] or on thermally tunable ring filters in a coupled-resonator optical waveguide (CROW) structure [3], both requiring sophisticated control schemes.

In this paper, we propose and experimentally demonstrate an OAWM scheme that does not require any optical slicing filters – neither for the signal not for the LO. Instead, we use an array of IQR, which are fed by the full optical waveform and by time-delayed copies of the full LO comb. The electrical signals then contain superimposed mixing products of the various LO tones with the respective adjacent portions of the signal spectra. For proper choice of the time delays, these superpositions are linearly independent and can thus be separated by DSP. As a base of our signal-processing scheme, we develop a precise frequency-domain model of our system that accounts for the complex-valued transfer functions of the various detection paths and that relies on a one-time calibration using a femtosecond laser with a known pulse shape. We demonstrate the viability of the scheme in a proof-of-concept experiment, in which we simultaneously acquire 16QAM and 64QAM wavelength-division multiplexing (WDM) channels, reaching overall detection bandwidths of more than 600 GHz. To the best of our knowledge, this is the highest bandwidth that has so far been demonstrated in an OAWM experiment.

2. Concept of slice-less optical arbitrary waveform measurement (OAWM)

The fundamental concept of a slice-less OAWM system is depicted in Fig. 1(a). The optical arbitrary waveform $a_\mathrm{S}(t)$ with spectrum $\underline{\tilde{a}}_\mathrm{S}(f)$ is split into N copies, which are fed to an array of parallel IQ receivers IQR ν, $\nu = \{1,\ldots,N\}$. The IQR are fed with time-delayed copies (delays τ_ν) of an LO comb comprising M phase-locked tones at optical frequencies f_μ, $\mu = 1,\ldots,M$, separated by a free spectral range (FSR) f_FSR, see Fig. 1(b). Each IQR comprises a 90° optical hybrid and two balanced photodetectors and is read out by a pair of ADCs with bandwidth B. In each of the N IQR, the full signal is mixed with all comb tones such that the baseband photocurrent of each IQR contains various mixing products of each LO tone with the respective adjacent spectral portion of the signal, see Fig. 1(c). For a given IQR ν, each of these M mixing products is subject to an individual baseband transfer function $\underline{\tilde{H}}_{\nu,\mu}(f)$, which accounts for the different time delays τ_ν, the amplitude and phase of the corresponding comb tone at frequency f_μ, as well as for the frequency-dependent transfer characteristics of the corresponding photodetectors and ADCs, see Fig. 1(c). The overall output signal $\underline{\tilde{U}}_\nu(f)$ of IQR ν is formed by a linear superposition of all these mixing products $\sum_\mu \underline{\tilde{H}}_{\nu,\mu}(f)\underline{\tilde{a}}_\mathrm{S}(f+f_\mu)$, Fig. 1(d). Accounting for an additional noise contribution $\underline{\tilde{A}}_{\mathrm{n},\nu}(f)$ at each IQR, the N output signals can be written as

$$\underbrace{\begin{bmatrix} \underline{\tilde{U}}_1(f) \\ \vdots \\ \underline{\tilde{U}}_N(f) \end{bmatrix}}_{\underline{\tilde{\mathbf{U}}}(f)} = \underbrace{\begin{bmatrix} \underline{\tilde{H}}_{1,1}(f) & \cdots & \underline{\tilde{H}}_{1,M}(f) \\ \vdots & \ddots & \vdots \\ \underline{\tilde{H}}_{N,1}(f) & \cdots & \underline{\tilde{H}}_{N,M}(f) \end{bmatrix}}_{\underline{\tilde{\mathbf{H}}}(f)} \underbrace{\begin{bmatrix} \underline{\tilde{a}}_\mathrm{S}(f+f_1) \\ \vdots \\ \underline{\tilde{a}}_\mathrm{S}(f+f_M) \end{bmatrix}}_{\underline{\tilde{\mathbf{A}}}_\mathrm{S}(f)} + \underbrace{\begin{bmatrix} \underline{\tilde{A}}_{\mathrm{n},1}(f) \\ \vdots \\ \underline{\tilde{A}}_{\mathrm{n},N}(f) \end{bmatrix}}_{\underline{\tilde{\mathbf{A}}}_\mathrm{n}(f)}. \tag{1}$$

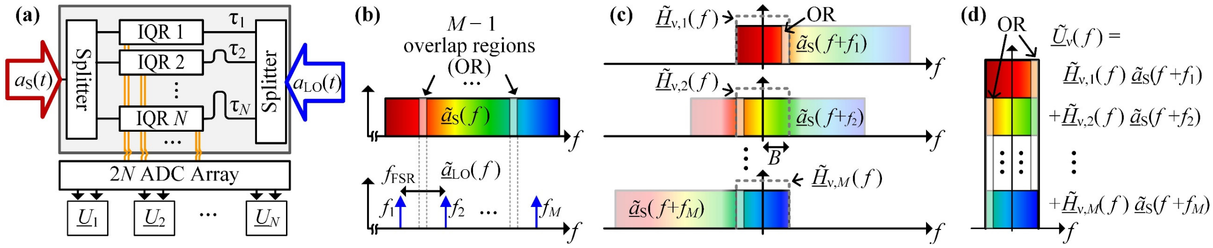

Fig. 1. Concept of slice-less optical arbitrary waveform measurement (OAWM). **(a)** Schematic setup: The arbitrary waveform $a_S(t)$ is split into N copies and fed to an array of in-phase/quadrature receivers (IQR). The local oscillator (LO) $a_{LO}(t)$ is also split into N copies, delayed by time delays τ_ν, $\nu=1,\dots N$, and fed to the IQR array. Each IQR is read out by a pair of analog-to-digital converters (ADC) with bandwidth B to obtain N complex baseband signals $\underline{U}_\nu(t)$. **(b)** Spectrum $\underline{\tilde{a}}_S(f)$ of arbitrary waveform $a_S(t)$ (top), and spectrum $\underline{\tilde{a}}_{LO}(f)$ of LO $a_{LO}(t)$ (bottom) with locked tones at frequencies f_μ, $\mu=1,\dots M$ and free spectral range f_{FSR}. Assuming $B > f_{FSR}/2$ there are $M-1$ overlap regions (OR) $[f_{\mu+1}-B, f_\mu+B]$, in which spectral components of the signal mix down with both adjacent comb lines to baseband frequencies smaller than B, see (c) and (d). **(c)** Visualization of the different mixing products generated in IQR ν and of the baseband transfer functions $\underline{\tilde{H}}_{\nu,\mu}(f)$ that account for electrical and optical characteristics of the system as well as for the amplitude and phase of the LO tone at frequency f_μ **(d)** Baseband spectrum $\underline{\tilde{U}}_\nu(f)$, consisting of a superposition of the various mixing products.

For simplicity, we assume that the noise contributions $\underline{\tilde{A}}_{n,\nu}(f)$ are statistically independent and spectrally white. For a known matrix $\underline{\tilde{\mathbf{H}}}(f)$, we can then obtain an estimate $\underline{\tilde{\mathbf{A}}}_S^{(est)}(f)$ of the various frequency-shifted copies of the original signal $\underline{\tilde{a}}_S(f+f_\mu)$ by multiplying the vector $\underline{\tilde{\mathbf{U}}}(f)$ of received base-band signals with the pseudo-inverse $(\underline{\tilde{\mathbf{H}}}^\dagger\underline{\tilde{\mathbf{H}}})^{-1}\underline{\tilde{\mathbf{H}}}^\dagger$ of the transfer matrix $\underline{\tilde{\mathbf{H}}}(f)$,

$$\underline{\tilde{\mathbf{A}}}_S^{(est)}(f) = \left(\underline{\tilde{\mathbf{H}}}^\dagger(f)\underline{\tilde{\mathbf{H}}}(f)\right)^{-1}\underline{\tilde{\mathbf{H}}}^\dagger(f)\underline{\tilde{\mathbf{U}}}(f) \quad . \tag{2}$$

Note that the pseudo-inverse $(\underline{\tilde{\mathbf{H}}}^\dagger\underline{\tilde{\mathbf{H}}})^{-1}\underline{\tilde{\mathbf{H}}}^\dagger$ can only be calculated if $N \geq M$, where M denotes the number of comb lines that lead to detectable mixing products with some spectral portion of the signal. For strictly band-limited signals, the overall comb may contain more than M comb lines as long as the associated mixing products are not captured by any IQR. Note also that the reconstruction according to Eq. (2) only works if the transfer matrix $\underline{\tilde{\mathbf{H}}}(f)$ is well-conditioned, which is the case for frequencies f within the bandwidth B of the IQR, $|f| < B$. For $|f| > B$, the individual matrix components become very small while the received baseband signals $\underline{\tilde{U}}_\nu(f)$ are strongly impaired by noise, thus rendering reliable reconstruction impossible.

For a practical realization of the filter-less OAWM system, the frequency-dependent transfer matrix $\underline{\tilde{\mathbf{H}}}(f)$ must be determined, which requires an independent calibration measurement of the system. Importantly, the transfer functions $\underline{\tilde{H}}_{\nu,\mu}(f)$ are impacted by amplitude and phase drifts of the comb lines and by random phase drifts in the setup. For Kerr combs pumped with highly stable lasers, the optical linewidth typically amounts to a few kHz [10], and mechanical vibrations in our setup are also limited to a similar frequency range. The associated amplitude and phase changes hence occur on time scales of hundreds of microseconds, and the transfer function $\underline{\tilde{\mathbf{H}}}(f)$ may be considered constant during one recording with a typical length of a few microseconds. This can be modeled by splitting each transfer-matrix element $\underline{\tilde{H}}_{\nu,\mu}(f)$ into a time-invariant, but frequency-dependent part $\underline{\tilde{H}}_{\nu,\mu}^{(f)}(f)$ and in a product of two frequency-independent parts $\underline{H}_{F,\nu}^{(t)}$ and $\underline{H}_{LO,\mu}^{(t)}$ that vary between different recordings,

$$\underline{\tilde{H}}_{\nu,\mu}(f) = \underline{\tilde{H}}_{\nu,\mu}^{(f)}(f) \times \underline{H}_{F,\nu}^{(t)} \times \underline{H}_{LO,\mu}^{(t)} , \tag{3}$$

where $\underline{H}_{F,\nu}^{(t)}$ accounts for the phase shift in the fiber leading to IQR ν and where $\underline{H}_{LO,\mu}^{(t)}$ represents the amplitude and phase fluctuation of the μ-th comb tone. For measuring the frequency-dependent part $\underline{\tilde{H}}_{\nu,\mu}^{(f)}(f)$, we perform a one-time calibration measurement in which we feed the system with a known reference waveform, derived from an ultra-stable femtosecond laser (MENHIR-1550) with well-defined pulse shape. The slowly drifting factors $\underline{H}_{F,\nu}^{(t)}$ and $\underline{H}_{LO,\mu}^{(t)}$ are estimated by exploiting the fact that the bandwidth B of each IQR is slightly larger than half the FSR, $B > f_{FSR}/2$, such that frequency components within the overlap regions $f_\mu^{(overlap)} \in [f_{\mu+1}-B, f_\mu+B]$, $\mu=1,\dots,M-1$, see Fig. 1(b), are reliably reconstructed twice in subsequent lines of the vector $\underline{\tilde{\mathbf{A}}}_S^{(est)}(f)$. This redundancy can be used to extract the frequency independent components $\underline{H}_{F,\nu}^{(t)}$ and $\underline{H}_{LO,\mu}^{(t)}$ in each recording and thus to reliably reconstruct the overall optical waveform $\underline{\tilde{a}}_S(f)$. Note that, for equidistant time delays τ_ν, the proposed OAWM scheme can be interpreted as optical time-domain sampling [4,5], provided that the frequency-dependent transfer function of the various detection channels and the phase drifts of the corresponding fiber links can be neglected. By exploiting the redundant information in the spectral overlap regions, the slice-less OAWM scheme described here can be used to measure truly arbitrary waveforms without restriction to data signals with known structure.

3. Experimental demonstration

We experimentally demonstrated the viability of the proposed OAWM scheme using discrete fiber-optic components. The LO tones are obtained by isolating four spectral lines from a dissipative Kerr soliton (DKS) comb. Variable optical delay lines are used to adjust the delays τ_ν to the various IQR. For IQR 1 we use balanced photodiodes (BPD) with a nominal 3 dB bandwidth of 43 GHz and an actual 12 dB bandwidth of approximately 80 GHz. For the remaining IQR the nominal BPD bandwidth is 100 GHz. The outputs of IQR 1 and IQR 2 are digitized with a 100 GHz oscilloscope (Keysight UXR1004A),

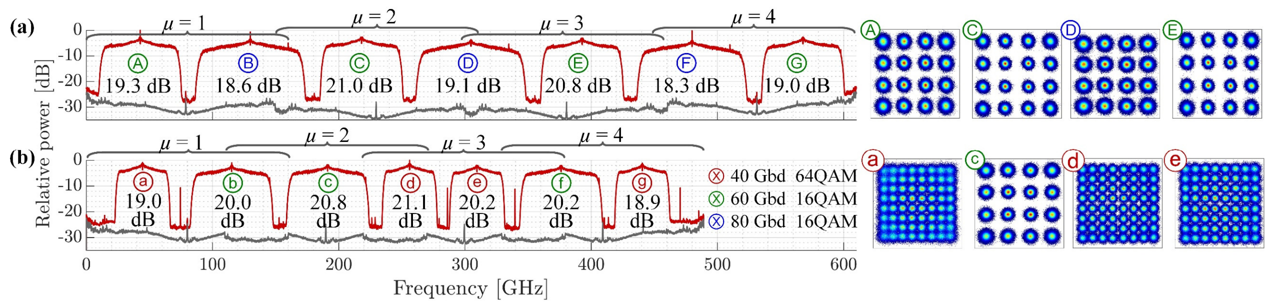

Fig. 2. Measurement results obtained in an optical back-to-back experiment with a local oscillator (LO) comb with an FSR of 150 GHz (a) or 110 GHz (b). Left: Normalized power spectrum of reconstructed waveform (red), which comprises four 60 GBd 16QAM signals (ⒶⒸⒺⒼ) and three 80 GBd 16QAM signals (ⒷⒹⒻ) (a), or four 40 GBd 64QAM signals (ⓐⓓⓔⓖ) and three 60 GBd 16QAM signals (ⓑⓒⓕ) (b). The spectrum of the transformed ADC noise floor (gray) increases to the edge of each spectral slice $\mu = 1,2,3,4$ due to the digital compensation of the receiver's bandwidth limitation but is reduced in the overlap region by averaging redundant signal components. The constellation signal-to-noise ratio (SNR) in dB is provided for all channels (Ⓐ-Ⓖ and ⓐ-ⓖ). Right: Exemplary constellation diagrams.

while for IQR 3 and IQR 4 we used an 80 GHz oscilloscope (Keysight UXR0804A). Both oscilloscopes are synchronized. For the DSP reconstruction, we limit the RF frequency range to B = 80 GHz for all channels.

In a first experiment, we use an FSR of 150 GHz, leading to 10 GHz-wide spectral overlap regions. Our LO comb features an optical carrier-to-noise power ratio (OCNR) between 25 dB and 27 dB, in a reference bandwidth of 12.5 GHz [11]. To test our system, we generate a WDM waveform by modulating four optical carriers with a 60 GBd 16QAM signal, ⒶⒸⒺⒼ in Fig. 2(a), and three carriers with an 80 GBd 16QAM signal, ⒷⒹⒻ in Fig. 2 (a). Prior to detection, we amplify the WDM signal with an erbium-doped fiber amplifier and remove out-of-band noise using an optical bandpass filter. The such prepared signal is received and digitally reconstructed with our system. Fig. 2(a) shows the spectrum of the reconstructed waveform as well as the transformed ADC noise floor. The latter is obtained by applying the same digital processing steps to pure ADC noise measurements. We mark the four overlapping spectral slices μ = 1,2,3,4 and specify the constellation signal-to-noise ratio (SNR) of the respective channels. Exemplary constellation diagrams are shown in the right-hand panel of Fig. 2. Note that the transformed ADC noise floor periodically increases toward the edges of the individual spectral slices, as we numerically compensate the roll-off of the detection system. Within the overlap regions, the ADC noise is reduced by averaging redundant spectral components. The overall constellation SNR of the outer spectral slices (μ = 1, μ = 4), is lower compared to the inner spectral slices (μ = 2, μ = 3), because the power of the associated LO tones are lower. Additional noise contributions arise due to an imperfect calibration, which leads to an imperfect separation of the spectral slices. Still, all signals are reconstructed with acceptable quality. To the best of our knowledge, the 600 GHz of spectral bandwidth covered in this measurement corresponds to the highest bandwidth that has so far been demonstrated in an OAWM experiment. In a second experiment, we reduce the FSR to 110 GHz, leading to 50 GHz-wide overlap regions and a total acquisition bandwidth of 490 GHz. In this experiment we used a combination of 40 Gbd 64QAM and 60 GBd 16QAM signals, covering a spectral range of 440 GHz, see Fig. 2(b). The constellation diagram exhibits some multiplicative noise, which we attribute to the rather low LO-comb OCNR of approx. 23 dB. Still, the 64QAM signals can be reliably reconstructed with acceptable quality.

4. Summary

We demonstrated an OAWM scheme that does not require any optical slicing filters – neither for the signal not for the LO. The scheme relies on a precise frequency-domain model of our system that accounts for the exact transfer functions of the various detection paths and that allows for acquisition of truly arbitrary waveforms. We demonstrate the viability of the scheme in proof-of-concept experiments, reaching record-high detection bandwidths of more than 600 GHz.

This work was supported by the ERC Consolidator Grant TeraSHAPE (# 773248), by the EU H2020 project TeraSlice (# 863322), by the DFG projects PACE (# 403188360) and GOSPEL (# 403187440) within the Priority Programme SPP 2111, by the BMBF project Open6GHub, by the EU H2020 Marie Skłodowska-Curie Innovative Training Network MICROCOMB (# 812818), by the Alfried Krupp von Bohlen und Halbach Foundation, by the Max-Planck School of Photonics (MPSP), and by the Karlsruhe School of Optics & Photonics (KSOP).

5. References

[1] Fontaine *et al.*, "Real-time full-field arbitrary optical waveform measurement," Nat. Photonics **4**, 248–254 (2010).
[2] Fontaine *et al.*, "228-GHz Coherent Receiver using Digital Optical Bandwidth Interleaving and Reception of 214-GBd (856-Gb/s) PDM-QPSK," ECOC 2012, Paper Th.3.A.1.
[3] Fang *et al.*, "Optical Arbitrary Waveform Measurement (OAWM) on the Silicon Photonic Platform," OFC 2021, Paper F2E.6.
[4] Fischer *et al.*, "High-Speed Digital Coherent Receiver Based on Parallel Optical Sampling," J. Light. Technol. **29**, 378–385 (2011).
[5] Chen *et al.*, "Coherent Detection Using Optical Time-Domain Sampling," IEEE Photon. Technol. Lett. **21**, 286–288 (2009).
[6] Proietti *et al.*, "Elastic Optical Networking by Dynamic Optical Arbitrary Waveform Generation and Measurement," J. Opt. Commun. Netw. **8**, A171-A179 (2016).
[7] Fang *et al.*, "320 GHz Analog-to-Digital Converter Exploiting Kerr Soliton Combs and Photonic-Electronic Spectral Stitching," ECOC 2021, Paper Th3C1-PD2.2
[8] Zazzi *et al.*, "Fundamental limitations of spectrally-sliced *optically* enabled data converters arising from MLL timing jitter," Opt. Express **28**, 18790–18813 (2020).
[9] Fontaine *et al.*, "Dynamic optical arbitrary waveform generation and detection in InP photonic integrated circuits for Tb/s optical communications," Opt. Comm. **284**, 3693–3705 (2011).
[10] Fuchuan Lei *et al.*, "Fundamental optical linewidth of soliton microcombs", arXiv 2102.05517 (2021).
[11] P. Marin-Palomo *et al.*, "Performance of chip-scale optical frequency comb generators in coherent WDM communications," Opt. Express **28**, 12897–12910 (2020).